Cyclodextrin mediated cholesterol extraction from lipid model membranes

Cesar A. López, Alex H. de Vries, Siewert J. Marrink

Supplementary information

Supplementary Methods

System set-up.

Three lipid models were used to represent biological membranes: diC_{16}-PC, SM and di$C_{18:2}$-PC. For the unbiased atomistic level extraction simulations, both small and larger systems were used. The small systems consisted of mixed monolayers of the following compositions: diC_{16}-PC-CHOL 1:1, 1:2, 1:3; SM-CHOL 1:1, 1:2, 1:3 and di$C_{18:2}$-PC-CHOL 1:1. In each case, nine β-CD dimers were placed with the hydroxyl groups in direct contact with the monolayer and solvated with a 4 nm water layer. A bigger system, consisting of 300 cholesterol molecules, 24 β-CDs, and 100 diC_{16}-PC molecules was set-up in a similar way, but only for the 1:3 diC_{16}-PC-CHOL system. In this case the β-CD were initially placed at a distance of 1.0 nm away from the monolayer surface either in monomeric or dimeric conformations (see Figure 1 in the main manuscript). For the free energy calculations, a range of additional small systems were used, consisting of a single β-CD dimer in direct contact with the monolayer. Similarly, three bilayer systems consisting of 4:1 (diC_{16}-PC, SM) and 10:1 (di$C_{18:2}$-PC) lipid/cholesterol ratio were prepared. Details of the system compositions, the simulation times, and number of repeats are given in Table S1. The small CG vesicle used in this study was formed by biased deformation of a lamellar lipid bilayer, as follows. The phase separated ($L_o - L_d$) CG lipid bilayer (see main text) was placed in a cubic box with edges 20% larger than the lateral edges of the membrane. The box was fully solvated with MARTINI water beads and fully equilibrated using an isotropic pressure approach. An external force was applied to the center of the bilayer to accelerate the sealing of the edges. A long equilibration time (40 μs) followed in order to re-equilibrate the distribution of the internal and external lipids (i.e. cholesterol can readily flipflop on this timescale), as well as the osmotic pressure. Afterwards, we added 98 β-CD dimers and 140 000 CG water beads in order to achieve an overall concentration of 0.04 M.

Computational details.

All-atom simulations were performed using a 2 fs time step to integrate Newton's equations of motion. The LINCS algorithm [1] was applied to constrain all bond lengths with a relative geometric tolerance of 10^{-4}. Non- bonded interactions were handled using a twin-range cutoff [2] scheme. Within a short-range cutoff of 0.9 nm, the interactions were evaluated every time step based on a pair list recalculated every five time steps. The intermediate-range interactions up to a long-range cutoff radius of 1.4 nm were evaluated simultaneously with each pair list update and were assumed constant in between. To account for electrostatic interactions beyond the long-range cutoff radius, a reaction field approach [3] was used with a relative dielectric permittivity of 66. Constant temperature was maintained by weak coupling of the solvent and solute separately to a Berendsen heat bath [4] with a relaxation time of 0.1 ps. Monolayers were coupled using an anisotropic scheme, maintaining a constant surface pressure of 33 mN m^{-1} (see next). Bilayers were coupled at 1.0 bar through a semiisotropic approach with relaxation time of 1.0 ps. Trajectories frames were stored every 40 ps. In the simulations at the CG level, we followed the standard simulation protocol used in the original version of the MARTINI model [5]. The non-bonded interactions are cutoff at a distance r_{cut} of 1.2 nm. To reduce the generation of unwanted noise, the standard shift function of GROMACS [6] is used in which both the energy and force smoothly vanish at the cutoff distance. The LJ and Coulomb potentials are shifted from r = 0.9 and r = 0.0 nm to the cutoff distance, respectively. The time step used to integrate the equations of motion is 20 fs. Constant temperature is maintained by weak coupling of the solvent and membranes separately to a Berendsen heat bath [4] with a relaxation time of 1.0 ps. The pressure of the planar

$L_o - L_d$ bilayer is maintained at 1.0 bar by weak semiisotropic coupling with a relaxation time of 1.0 ps. Finally, an isotropic pressure scheme was used during the simulation of the small vesicle.

Surface pressure calculation of lipid monolayers.

The surface tension in GROMACS [6] is calculated from the diagonal components of the pressure tensor:

$$\gamma_s = h_z(P_{zz} - \left(\frac{P_{zz} + P_{yy}}{2}\right)) \tag{1}$$

where h_z is the z-component of the box size. The quantity P_{zz} is the pressure normal to the monolayer and $\frac{P_{xx}+P_{yy}}{2}$ is the pressure tangential to the monolayer. The surface tension γ_s is the difference between these pressures. In our set-up, the monolayers are coupled to an effective surface tension of 77 mN m^{-1}, which is the sum of the surface tensions of lipid/water interface, γ_m, and the water/vacuum interface, γ_{wv}:

$$\gamma_s = \gamma_m + \gamma_{wv} \tag{2}$$

The surface pressure π was calculated from the surface tension through the following relation:

$$\pi = \gamma_{wv} + \gamma_m \tag{3}$$

Assuming a value $\gamma_{wv} = 55$ mN m^{-1}, previously calculated by Chen et al. [7] for the SPC water model being at 288 K, we obtain a constant surface pressure of 33 mN m^{-1} for the monolayers. The values for temperature as well as surface pressure are optimal for cyclodextrin mediated cholesterol extraction from cholesterol monolayers under experimental conditions [8].

Free energy calculation.

An umbrella sampling approach was used to calculate the potential of mean force (PMF) for a number of important sub-steps related to the total desorption process, namely i) the β-CD mediated extraction of one single cholesterol molecule from the monolayer/bilayer, ii) the extraction of cholesterol from the cholesterol-lipid monolayer to the water bulk, and iii) the desorption of a β-CD dimer from the bilayer interface to the water bulk. For the PMF calculations, we used the umbrella sampling method [9] with 25 window points, spaced by 1 Å, restraining the center of mass of one cholesterol with respect to the center of mass of the β-CD (i), between the center of mass of one single cholesterol to the center of mass of the monolayer (ii), and the center of mass of a β-CD dimer to the center of mass of the monolayer/bilayer (iii). The restraining potential was harmonic with a force constant of 1,000 kJ mol^{-1} nm^{-2}. 200 ns of simulation was performed for each window, see Table S2 for an overview. The PMFs were reconstructed using the weighted histogram analysis method [10], with 200 bins for each profile. To estimate the convergence in the PMF, the 200 ns of each window were divided in five blocks. The statistical error was calculated from the variance between averages over the individual blocks, and is less than 5 kJ mol^{-1} for all values reported.

CG CD model.

The β-CD molecule was initially parameterized using the carbohydrate MARTINI model [11]. The CG model represents an atomistic β-CD dimer in a head-head conformation, which we previously showed to be the optimal conformation for cholesterol extraction [12]. Every monosaccharide sub-unit was mapped as a three bead model and connected using the bonded potentials for the amylose chain [11]. Single rings were connected through bonds in order to represent the dimer. While the CG model preserves the structural conformation observed from the atomistic simulations, the model failed in reproducing the different thermodynamic sub-steps calculated with the atomistic model. Therefore a refinement of some of the non-bonded interactions was required. After iterative adjustment, we came up with a CG topology which reproduces the cholesterol extraction free energy landscape and the dimer desorption free energy from the lipid bilayer (Figure S7). In particular, we included a special bead "PC" which preserves the features of a MARTINI P4 bead, except for its interaction with water beads. The PC-P4 interaction level was decreased to the semi-attractive level, with LJ parameters $\varepsilon = 4.0$ kJ mol^{-1} and $\sigma = 0.47$ nm. To account for the loss of available H-bonds upon formation of the dimer, the polarity of the central beads was somewhat reduced to the level of a C5 particle. The final topology is shown in Figure S7C.

Supplementary Results.

Cyclodextrin desorption from bilayer interface.

An important key step in the cholesterol extraction process is the affinity of the cyclodextrin dimer for the membrane. Our supporting energetic calculations, shown in Figure S5, suggest that (i) the cyclodextrin dimer has a strong affinity for the lipid bilayer, with a binding free energy of about 35 kJ mol^{-1}, and (ii) does not have a preference for any particular bilayer composition. However, the dimer can interact deeper at less energetic cost with membranes composed of unsaturated lipids, which may increase the probability of having a cholesterol closer to the CD cavity.

Temperature effect on cholesterol extraction by Cyclodextrin

PMFs of cholesterol extraction from both Lo and Ld mimetic bilayers were also probed at 310 K. The resulting PMFs (Fig. S6) show that the main features do not change upon raising the temperature. However, the barrier and extraction energy seem to be affected in the order of 10 kJ mol^{-1}. These data point to an increased cholesterol desorption rate at higher temperature, as a result of the decrease in cholesterol shielding by the lipids of the membrane.

References

[1] Hess, B.; Bekker, H.; Berendsen, H. J. C.; Fraaije, J. *J. Comput. Chem.* **1997**, *18*, 1463–1472.

[2] van Gunsteren, W. F.; Berendsen, H. J. C. *Angew. Chem. Int. Ed.* **1990**, *29*, 992–1023.

[3] Tironi, I.; Sperb, R.; Smith, P.; van Gunsteren, W. F. *J. Chem. Phys.* **1995**, *102*, 5451–5459.

[4] Berendsen, H. J. C.; Postma, J. P. M.; van Gunsteren, W. F.; Dinola, A.; Haak, J. R. *J. Chem. Phys.* **1984**, *81*, 3684–3690.

[5] Marrink, S. J.; Risselada, H. J.; Yefimov, S.; Tieleman, D. P.; de Vries, A. H. *J. Phys. Chem. B* **2007**, *111*, 7812–7824.

[6] Hess, B.; Kutzner, C.; van der Spoel, D.; Lindahl, E. *J. Chem. Theory Comput.* **2008**, *4*, 435–447.

[7] Chen, F.; Smith, P. E. *J. Chem. Phys.* **2007**, *126*, 221101–221101.

[8] Ohvo, H.; Slotte, J. P. *Biochemistry* **1996**, *35*, 8018–8024.

[9] Torrie, G.; Valleau, J. *J. Comput. Phys.* **1977**, *23*, 187–199.

[10] Kumar, S.; Rosenberg, J.; Bouzida, D.; Swendsen, R.; Kollman, P. *J. Comput. Chem.* **1992**, *13*, 1011–1021.

[11] López, C. A.; Rzepiela, A. J.; de Vries, A. H.; Dijkhuizen, L.; Hünenberger, P. H.; Marrink, S. J. *J. Chem. Theory Comput.* **2009**, *5*, 3195–3210.

[12] López, C. A.; de Vries, A. H.; Marrink, S. J. *PLoS Comput. Biol.* **2011**, *7*, 1–11.

Table S1. Overview of simulations

Unbiased simulations	Composition	Sim. time (ns)	Repeats	Chol. extracted	Extr. rates (chol CD^{-1} ns^{-1})	Extr. time (ns)
diC_{16}-PC-CHOL $1{:}1_{mon}$	70 diC_{16}-PC, 70 CHOL, 9 CDs dimers	200	5	-	-	-
diC_{16}-PC-CHOL $1{:}2_{mon}$	25 diC_{16}-PC, 50 CHOL, 9 CDs dimers	200	3	-	-	-
diC_{16}-PC-CHOL $1{:}3_{mon}$	25 diC_{16}-PC, 75 CHOL, 9 CDs dimers	200	3	8	0.0007	20-50
diC_{16}-PC-CHOL $1{:}3_{mon}$	100 diC_{16}-PC, 300 CHOL, 12 CDs dimers	500	2	5	0.0002	50
diC_{16}-PC-CHOL $1{:}3_{mon\text{-}big}$	100 diC_{16}-PC, 300 CHOL, 24 CDs monomers	500	2	-	-	-
SM-CHOL $1{:}1_{mon}$	70 SM, 70 CHOL, 9 CDs dimers	200	4	-	-	-
SM-CHOL $1{:}2_{mon}$	31 SM, 59 CHOL, 9 CDs dimers	400	5	4	0.0001	50-300
SM-CHOL $1{:}3_{mon}$	25 SM, 75 CHOL, 9 CDs dimers	300	4	8	0.0004	30-300
$diC_{18:2}$-PC-CHOL $1{:}1_{mon}$	70 $diC_{18:2}$-PC, 70 CHOL, 9 CDs dimers	300	7	2	0.00005	300
CG bilayer	769 SM, 507 $diC_{18:2}$-PC, 538 CHOL, 20 CDs dimers	10^4	10	11	2x10^{-6} (L_d), 7.5x10^{-7} (L_o)	10^3-10^4
CG vesicle	769 SM, 507 $diC_{18:2}$-PC, 538 CHOL, 98 CDs dimers	2*10^4	1	11	4x10^{-6} (L_d), 1.5x10^{-6} (L_o)	10^2-10^4

Biased simulations (PMFs)	Composition	Event	Time	Windows
diC_{16}-PC-CHOL $4{:}1_{mon}$	64 diC_{16}-PC, 16 CHOL	a^*	200	25
diC_{16}-PC-CHOL $1{:}1_{mon}$	70 diC_{16}-PC, 70 CHOL	a	200	25
diC_{16}-PC-CHOL $1{:}2_{mon}$	25 diC_{16}-PC, 50 CHOL	a, $c^\dagger$	200, 200	25, 25
diC_{16}-PC-CHOL $1{:}3_{mon}$	25 diC_{16}-PC, 75 CHOL	a, c	200, 200	15, 25
SM-CHOL $1{:}1_{mon}$	70 SM, 70 CHOL	a	200	25
SM-CHOL $1{:}2_{mon}$	31 SM, 59 CHOL	a, c	200, 200	25, 25
SM-CHOL $1{:}3_{mon}$	25 SM, 75 CHOL	a, c	200, 200	15, 25
$diC_{18:2}$-PC-CHOL $4{:}1_{mon}$	64 $diC_{18:2}$-PC, 17 CHOL	a	200	25
$diC_{18:2}$-PC-CHOL $1{:}1_{mon}$	70 $diC_{18:2}$-PC, 70 CHOL	a	200	25
diC_{16}-PC-CHOL $3{:}1_{bila}$	160 diC_{16}-PC, 42 CHOL	a, $b^\ddagger$	200, 200	25, 23
SM-CHOL $3{:}1_{bila}$	164 SM, 44 CHOL	a, b	200, 200	25, 23
$diC_{18:2}$-PC-CHOL $10{:}1_{bila}$	128 $diC_{18:2}$-PC, 12 CHOL	a, b	200, 200	25, 23
CG diC_{16}-PC-CHOL-$3{-}1_{bila}$	160 diC_{16}-PC, 42 CHOL	a, b	200, 200	25, 23

*βCD mediated cholesterol extraction

†unassisted cholesterol extraction

‡βCD dimer desorption

Table S2. Overview of the energetic characterization of the CD mediated cholesterol extraction.[§]

System	$\triangle G^{extr*}$ (kJ mol^{-1})	$\triangle G^{bar\dagger}$ (kJ mol^{-1})
CHOL[‡]	40	0
diC$_{16}$-PC/CHOL 4:1	5	65
diC$_{16}$-PC/CHOL 3:1	10	60
diC$_{16}$-PC/CHOL 1:1	20	40
diC$_{16}$-PC/CHOL 1:2	45	20
diC$_{16}$-PC/CHOL 1:3	40	10
diC$_{16}$-PC/CHOL 3:1$_{bilayer}$	10	70
SM-CHOL 3:1	20	60
SM-CHOL 1:1	20	50
SM-CHOL 1:2	50	5
SM-CHOL 1:3	60	0
SM-CHOL 3:1$_{bilayer}$	0	80
diC$_{18:2}$-PC 10:1	30	30
diC$_{18:2}$-PC 4:1	45	25
diC$_{18:2}$-PC 1:1	30	30
diC$_{18:2}$-PC 10:1$_{bilayer}$	30	40

[*] corresponds to the free energy difference between the membrane-bound and CD-complexed states.

[†] denotes the free energy difference between the membrane-bound state and the state of largest free energy along the extraction pathway.

[‡] The values for the pure CHOL monolayer were taken from [12].

[§] errors 5 kJ mol^{-1} at most.

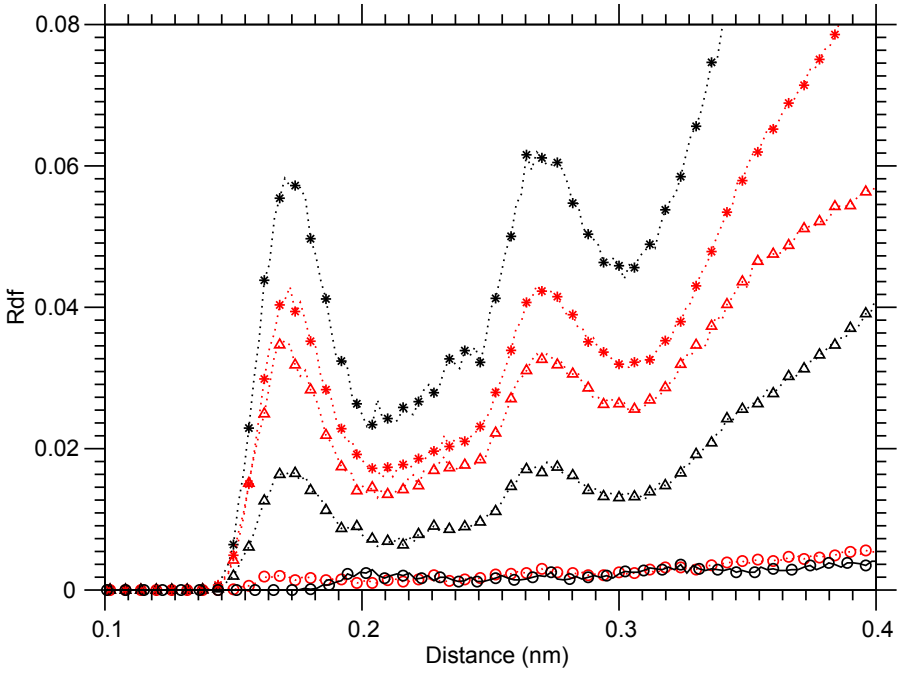

Fig. S1. Structural characterization of membrane-CD interaction through radial distribution functions (RDFs). RDFs between β-CDs and the surface of the monolayers were calculated for diC$_{16}$-PC/CHOL (black lines) and SM/CHOL (red lines) at 1:1 (open circles), 1:2 (triangles up) and 1:3 (stars) molar ratio, respectively. RDFs were calculated between the OH groups of cholesterol molecules and the center of mass of the CDs.

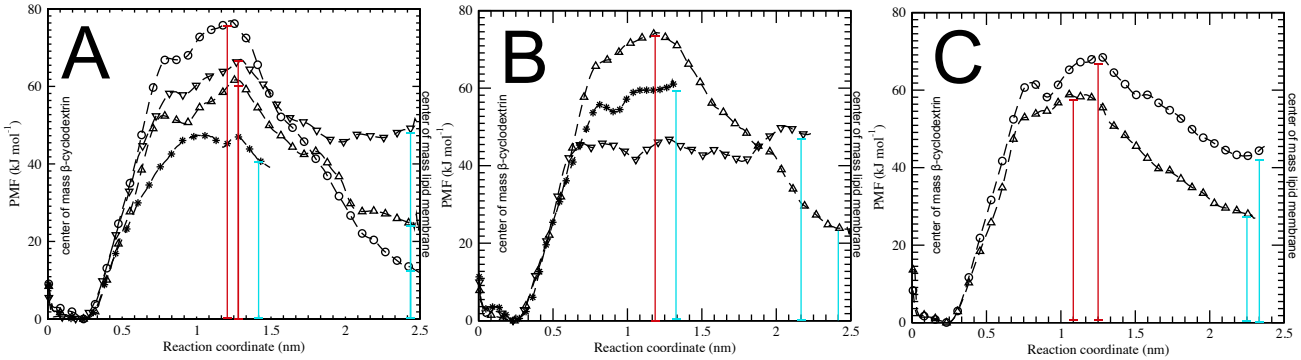

Fig. S2. Energetic characterization of cholesterol extraction through potential of mean force (PMF). The reaction coordinate represents the difference between the center-of-masses of the extracted cholesterol and the β-CD dimer. A distance of 0 nm corresponds to the cholesterol complexed with β-CD, the largest distance indicates full embedding of cholesterol in the monolayer. Cyan and red bars denote the reference points for calculating ΔG^{bar} and ΔG^{extr} respectively (see Figure 3 in the main manuscript). PMFs were calculated for (A) diC_{16}-PC-CHOL monolayers with molar ratios varying from 4:1 (open circles) to 1:1 (triangles up), 1:2 (triangles down) and 1:3 (stars); (B) SM-CHOL at ratios 1:1 (triangles up), 1:2 (triangles down),1:3 (stars) and (C) di$C_{18:2}$-PC-CHOL at ratios 4:1 (open circles) and 1:1 (triangles up) respectively.

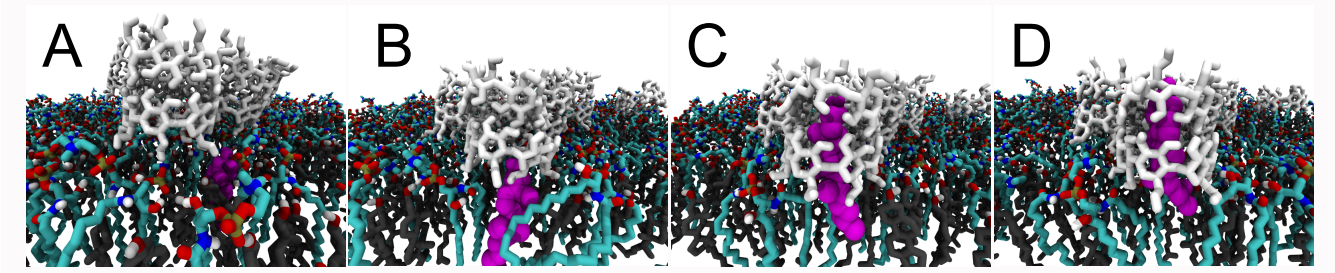

Fig. S3. Spontaneous extraction of cholesterol from a SM-CHOL 1:2 monolayer by cyclodextrin dimers. Panel (A) shows the initial system set-up with β-CD dimers sitting on top of the monolayer, panels B-D show the evolution of the extraction of cholesterol by one of the β-CD dimers. The β-CDs interact with the lipid head groups only and the cholesterol is still inside the monolayer (B), the β-CD is embedded more deeply and the upper part of cholesterol is sucked in (C), followed by the rapid complexation of cholesterol by the β-CD dimer (D). The whole extraction process takes place within 50-300 ns (over 5 independent simulations). Color code; SM tails: cyan, SM head group: red, blue and cyan, cholesterol body: grey, cholesterol head: red-white, cholesterol extracted: magenta, CDs: white. Water is not depicted.

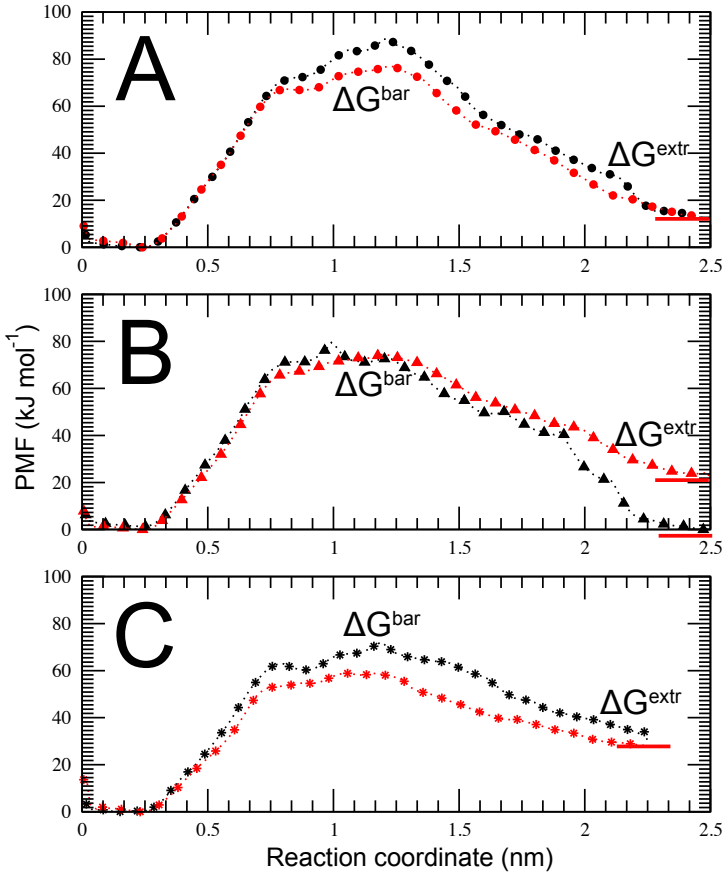

Fig. S4. PMF for β-CD mediated cholesterol extraction from lipid bilayer (black line) versus monolayer (red line) model membranes. Reaction coordinate as in Figure S2. Results are shown for diC_{16}-PC/CHOL 3:1 (A), SM/CHOL 3:1 (B), and di$C_{18:2}$-PC 10:1 (C) membranes.

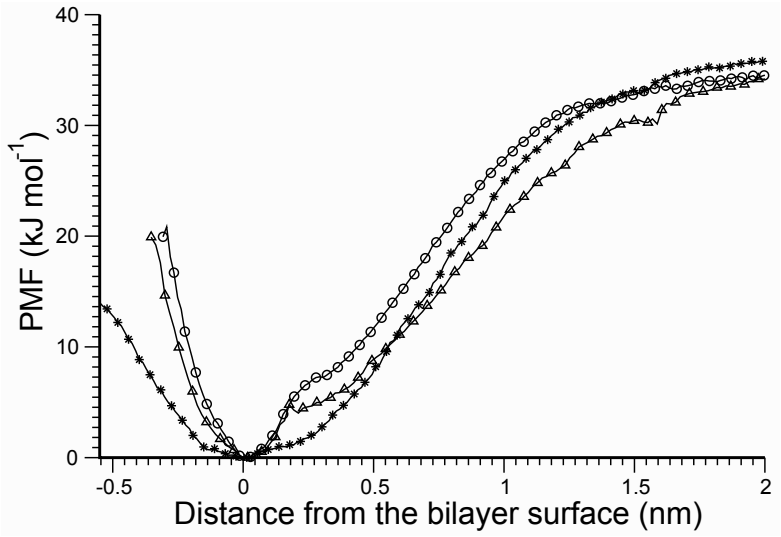

Fig. S5. Energetic characterization of β-CD desorption from different lipid model membranes. A single β-CD dimer was placed close to the water-membrane interface and the PMFs for the desorption from a diC_{16}-PC/CHOL 3:1 (up-triangles), SM/CHOL 3:1 (open circles) and di$C_{18:2}$-PC/CHOL 10:1 (stars) bilayer were calculated. The reaction coordinate represents the distance between the center-of-mass of the β-CD and the center-of-mass of the lipid bilayer. The reaction coordinate was shifted such that 0.0 nm corresponds to the membrane-adsorbed equilibrium position.

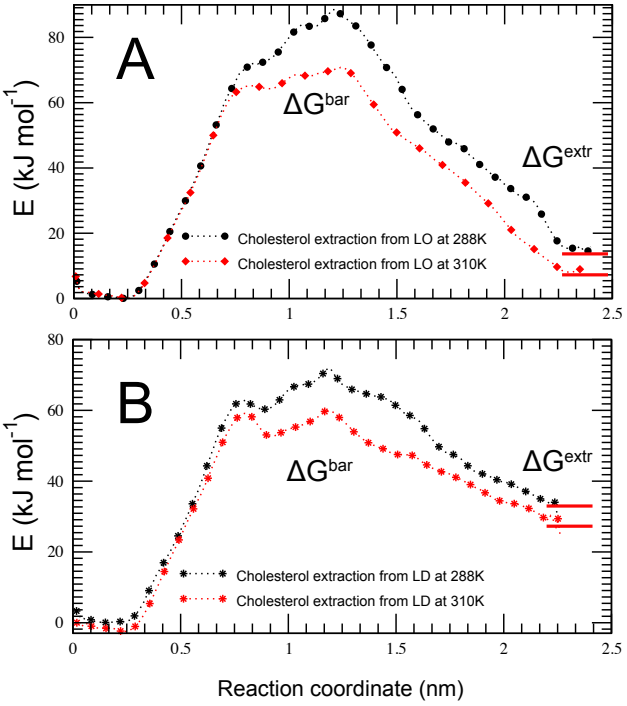

Fig. S6. PMF for β-CD mediated cholesterol extraction from lipid model membranes at 288K (black lines) and 310K (red lines). Reaction coordinate as in Figure S2. Results are shown for Lo mimicking bilayer diC_{16}-PC/CHOL 3:1(A), and Ld mimicking bilayer di$C_{18:2}$-PC 10:1 (B) membranes.

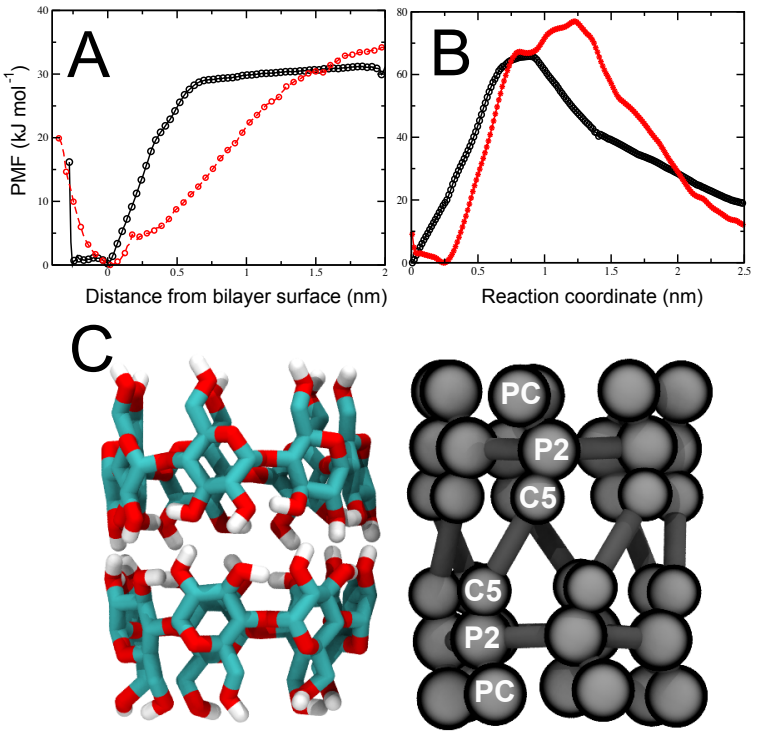

Fig. S7. Comparison of PMFs between all atom (red) and CG model (black). Iterative parameterization of the CD CG model was carried out in order to reproduce the free energies of CD desorption as well as CD-mediated extraction of cholesterol from a lipid bilayer. (A) PMF of the desorption of a CD dimer from a diC_{16}-PC bilayer. Although the slopes of the PMFs are different, the end points (i.e. the desorption free energies) are similar to within 5 kJ mol^{-1}. Reaction coordinate as in Figure S5. (B) PMF of cholesterol extraction from a diC_{16}-PC/CHOL 3:1 bilayer, showing qualitative similar extraction profiles and an overall free energy gain of around 20 kJ mol^{-1} in both cases. Reaction coordinate as in Figure S2. (C) Atomistic and MARTINI CG representation of the β-CD head-head dimer. A special "PC" bead was included which interacts through a semi-attractive level with the MARTINI water beads.